DOI: 10.15669/pnst.8.268

Progress in Nuclear Science and Technology
Volume 8 (2025) pp. 268-273

ARTICLE

Separation of Minor Actinides and Lanthanides from High-Level Liquid Waste using CMPO-Impregnated Adsorbent

Riho OKAJIMA [1,2], Masahiko KUBOTA [1] and Seong-Yun KIM [1*]

[1] *Department of Quantum Science and Energy Engineering, Graduate School of Engineering, Tohoku University, Sendai, Miyagi, 980-8579, Japan*
[2] *Japan Nuclear Fuel Limited, Rokkasho, Kamikitagun, Aomori, 039-3212, Japan*

To separate trivalent minor actinides and lanthanides from high-level liquid waste (HLLW), an octyl(phenyl)-*N*,*N*-diisobutylcarbamoyl methylphosphine oxide (CMPO)–impregnated adsorbent was synthesized by impregnating microporous silica particles with the CMPO extractant. The morphology of the adsorbent was characterized via scanning electron microscopy-energy-dispersive X-ray and thermogravimetric analyses. The adsorption ability of the synthesized adsorbent for Ln(III) was constant at HNO_3 concentrations of 0.1–0.5 M, whereas the adsorption of Zr(IV), Mo(VI), and Re(VII) was affected by the HNO_3 concentration. The adsorption performance of the CMPO adsorbent for Eu(III) in the solid state was studied using particle-induced X-ray emission and X-ray photoelectron spectroscopy (XPS). The depth-profiling XPS results and slope analysis revealed the formation of a complex of Eu and CMPO with a 1:3 coordination structure. The selective stripping of the adsorbed ^{241}Am, ^{152}Eu, Zr(IV), and Mo(VI) from simulated HLLW was successfully achieved using column chromatography.

KEYWORDS: high-level liquid waste, impregnated adsorbent, adsorption, separation

I. Introduction

Owing to the increasing electricity consumption associated with the continuous industrial development, nuclear power generation is being adopted in countries around the world to ensure a stable electricity supply.[1-2] Compared with other methods of power generation, nuclear power generation can produce a large amount of electricity; however, the concomitantly increasing amount of spent nuclear fuel generated after power generation is a pressing concern.

Spent nuclear fuel can be reprocessed using the PUREX method, which allows U and Pu to be extracted and reused as fuel. However, spent nuclear fuel contains many nuclides with long-term radiation toxicity, such as minor actinides (MA(III)) with long half-lives, whose efficient separation is a challenging task. [3)]

To solve this important technical problem, intense research efforts are being devoted to the development of extraction chromatography methods using porous silica adsorbents impregnated with extractants.[4)] In particular, composite carrier particles composed of porous silica particles containing styrene–divinylbenzene copolymer in the pores (SiO_2-P) exhibit excellent resistance to HNO_3 and are promising research targets for improving resistance to radiation.

However, MA(III) has very similar chemical properties to lanthanides (Ln(III)), which renders their mutual separation extremely difficult. Therefore, the selective separation of MA(III) from Ln(III) is the most important technical issue in high-level liquid waste (HLLW) treatment.

Various extractants have been developed and studied for selectively recovering MA(III),[5)] including TODGA,[6)] TEHDGA,[7)] TRPO,[8)] and BTBP.[9)] However, because HLLW has a high acid concentration and many nuclides, the separation of MA(III) from HLLW suffers from selectivity issues. In this context, octyl(phenyl)-*N*,*N*-diisobutylcarbamoyl methylphosphine oxide (CMPO) has emerged as an effective extractant for the selective separation of MA(III) and Ln(III) from highly acidic solutions.[10-12)] However, further knowledge on the adsorption and separation characteristics as well as on the binding mode of CMPO with metals and the adsorption distribution within impregnated adsorbents is required to realize the practical application of CMPO as an extractant of MA(III) and Ln(III) in HLLW treatment plants.

Previous studies have investigated the separation performance of metal ions on CMPO/SiO_2-P adsorbents, however, the exact adsorption behavior in the solid phase has not been fully understood. Furthermore, the impact of the adsorbent on the adsorption and separation performance of MA(III) and Ln(III) under specific metal ion conditions remains insufficiently explored. In view of these gaps, the aim of this research is to elucidate the solid-phase metal ion adsorption behavior of the CMPO/SiO_2-P adsorbent for MA(III) and Ln(III), and to investigate the adsorption and separation performance of the column in simulated HLLW spiked with ^{241}Am and ^{152}Eu. First, the adsorption performance of each metal ion on the prepared CMPO/SiO_2-P adsorbent was evaluated by performing a series of batch experiments, and the effect of the HNO_3 concentration

*Corresponding author, E-mail: sonyun.kimu.d7@tohoku.ac.jp

behavior was evaluated. Furthermore, to confirm the adsorption behavior of Eu(III) on the CMPO adsorbent, particle-induced X-ray emission (PIXE), X-ray photoelectron spectroscopy (XPS), and slope analysis were performed. In addition, column separation experiments were conducted using simulated solutions containing MA(III), and the column separation performance for MA(III) and Ln(III) was evaluated.

II. Experimental

1. Materials

The simulated HHLW used in the batch and column experiments was prepared using individual reagents to include 15 types of metal ions. $Cs(I)NO_3$, $Sr(II)(NO_3)_2$, $Ba(II)(NO_3)_2$, and $RE(NO_3)_3{\cdot}6H_2O$ (RE = La(III), Ce(III), Nd(III), Sm(III), Eu(III) and Gd(III) were purchased from Kanto Chemical Co. Ru(III) $(NO)(NO_3)_3$, $Pd(II)(NO_3)_2$, and Rh(III) $(NO_3)_3$ nitrate solution were purchased from Sigma-Aldrich. $Zr(IV)O(NO_3)_2{\cdot}2H_2O$, $(NH_4)_6Mo(VI)_7O_{24}{\cdot}4H_2O$ were purchased from Kanto Chemical Co. Rhenium(VII) oxide was purchased from Mitsuwa Chemicals Co. The batch experiments and column experiments used a simulated HLLW containing 15 metal ions at 5 mM. The nitric acid solution composed of single metal ion Eu(III)was used for the experiment of Adsorption mechanism. The ^{241}Am (9.3 kBq/ml) and ^{152}Eu (102 kBq/ml) radioisotopes were used to evaluate the adsorption behavior for MA(III) and Ln(III) in column experiments. Concentrated nitric acid and deionised water were used to vary the nitric acid concentration of the simulated HLLW and the single metal ion nitric acid solution according to the experimental conditions.

The CMPO/SiO_2-P adsorbent was prepared by impregnating SiO_2-P particles with an average diameter of 40–60 μm and an average pore size of 50 nm with the CMPO extractant. Briefly, 10 g of CMPO was dissolved in dichloromethane and then mixed with 40 g of SiO_2-P. The mixture was stirred at room temperature for 1 h to allow impregnation. Subsequently, the dichloromethane was evaporated by gradually reducing the pressure at 40°C using a rotary evaporator, and the sample was dried overnight under vacuum.

2. Characterization

The surface morphology was examined using a scanning electron microscope (SEM, TM4000Plus) equipped with an energy-dispersive X-ray (EDX) analyzer. Thermogravimetric analysis (TGA) was conducted using a SHIMADZU DTG-60/60H by heating the samples from 25°C to 600°C at a rate of 1°C/min under a N_2 atmosphere (30 mL/min). A solid-state study of the behavior of the CMPO/SiO_2-P adsorbent before and after the adsorption experiments was performed with a 4.5 MeV dynamitron accelerator at Tohoku University. A 3 MeV proton beam focused to a spot size (of 1 × 1 μm^2) was applied to the target sample particles. The X-rays emitted by the elements adsorbed on the CMPO/SiO_2-P adsorbent were collected and subsequently analysed using GeoPIXE II software to construct elemental maps.

3. Batch Experiments

The adsorption performance of the prepared CMPO/SiO_2-P adsorbent was tested by varying the HNO_3 concentration while maintaining a constant temperature. Specifically, 0.2 g of CMPO/SiO_2-P and 4 mL of the simulated HLLW solution were placed in a glass vial and shaken mechanically at a specific contact time and a speed of approximately 160 rpm using a water bath shaker with temperature control (NTS-4000B, Tokyo Rika Kiki Co., Ltd., Japan). After shaking, phase separation was conducted using a syringe fitted with a nylon membrane filter with a pore size of 20 μm. The concentration of metal ions before and after adsorption was measured using inductive coupled plasma-atomic emission spectroscopy (ICP-AES, Thermo Fisher Scientific iCAP Pro XP Duo), and that of Cs(I) was determined using atomic absorption spectroscopy (AAS, SHIMADZU AA-6200). The uptake ratio (%) and distribution coefficient (K_d; ml/g) were calculated as follows:[13)]

$$Uptake\ ratio(\%) = \frac{(C_0 - C_e)}{C_0} \times 100$$

$$K_d = \frac{(C_0 - C_e)}{C_0} \times \frac{V}{m}$$

where C_0 and C_e (mM) represent the initial and equilibrium concentrations of each element, respectively, V is the volume of the solution (ml), and m is the mass of the CMPO/SiO_2-P adsorbent (g).

4. Column Experiments

The separation performance for ^{241}Am, ^{152}Eu, and other metal ions in simulated HLLW was evaluated via column chromatography. A column (10 mm diameter, 130 mm length) was packed with the adsorbent, which was previously degassed in water overnight. The simulated HLLW solution spiked with ^{241}Am and ^{152}Eu was used as the feed, 2 M HNO_3 was used as the wash solution, and water and 0.01 M diethylenetetraaminepentaacetic acid (DTPA) were used as the eluents. Each solution was fed at 0.5 ml/min, and the effluent was collected every 5 ml using a fraction collector (DC-1500, Tokyo Rikakikai Co., Ltd.). Using ICP-AES and AAS, the metal ion concentrations in the recovered solutions were measured as in the batch experiment. The recovery ratios of the metal ions were determined according to the total volume fractions of 2 M HNO_3, H_2O, and 0.01 M DTPA.

The radioactivity of ^{241}Am and ^{152}Eu was measured using a γ-ray spectrometer (Canberra Ge semiconductor detector), with detecting γ-rays at 59.5 keV for ^{241}Am and 122 keV for ^{152}Eu. The measurement data were analyzed using Canberra software (Genie 2000). The radioactivity concentrations in the collected solutions were determined, and the adsorption and elution performances were evaluated using the decontamination factor (DF) as follows:[14)]

$$DF = \frac{(C_{feed} \times V_{feed})}{C_{product} \times V_{product}}$$

where C_{feed} and $C_{product}$ are the metal concentrations

in the feed and product solutions, and V_{feed} and $V_{product}$ are the corresponding volumes. The product fraction was defined as the volume fraction of H_2O in the interval where ^{241}Am was eluted, and the corresponding DF values were calculated.

III. Results and Discussion

1. Surface Observation and Impregnation Ratio Analysis of the Adsorbent

Figures 1(a) and **1(b)** display SEM images of SiO_2-P before and after impregnation with CMPO, respectively. The smooth surface and absence of uneven CMPO deposition indicate the successful impregnation of CMPO into the SiO_2-P particles. **Figure 2** illustrates the TGA curves of CMPO/SiO_2-P and its constituent materials. The thermal decomposition of CMPO started at around 200°C. At approximately 300°C, a substantial weight loss was observed for SiO_2-P, which can be attributed to the combustion of the styrene–divinylbenzene copolymer embedded within the pores of the SiO_2 particles. The composition ratios of SiO_2-P particles, styrene–divinylbenzene copolymer, and CMPO in the CMPO/SiO_2-P adsorbent were calculated on the basis of the TGA results (**Table 1**). The obtained ratios closely match the targeted synthesis composition of CMPO/SiO_2-P, confirming the successful synthesis of the CMPO/SiO_2-P adsorbent.

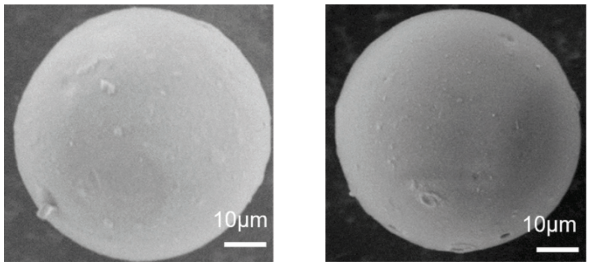

(a) (b)

Fig. 1 SEM images of (a) SiO_2-P and (b) the CMPO/SiO_2-P adsorbent

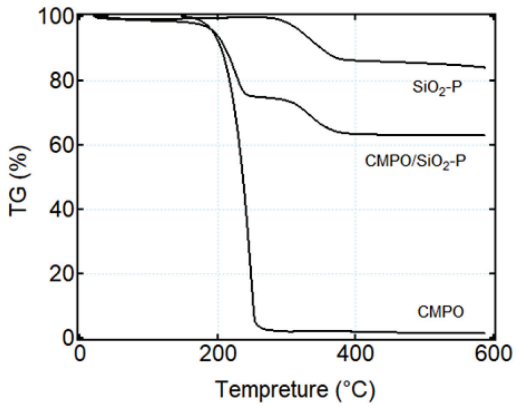

Fig. 2 Thermogravimetric curves of SiO2-P, CMPO, and the CMPO/SiO2-P adsorbent (atmosphere: N2 gas, heating rate: 1°C/min)

Table 1 Weight composition of SiO_2-P and the CMPO/SiO_2-P adsorbent obtained via thermogravimetric analysis

	Conditions of synthesis		
	SiO_2 (wt.%)	SDB (wt.%)	Extractant (wt.%)
SiO_2-P	81.6	18.4	
CMPO/SiO_2-P	65.3	14.7	20.0
	Thermal analysis		
CMPO/SiO_2-P	65.1	11.4	23.5

2. Effect of HNO_3 Concentration

Figure 3 illustrates the adsorption ratio of CMPO/SiO_2-P in HNO_3 solutions with concentrations ranging from 0.1 to 5 M. For Ln(III) ions, the CMPO/SiO_2-P adsorbent exhibited adsorption ratios between 10% and 20% regardless of the HNO_3 concentration. In contrast, the adsorption behavior for other metal ions, particularly Zr(IV) and Mo(VI), demonstrated notable selectivity. The adsorption ratios for these elements increased with increasing HNO_3 concentration, reaching approximately 80% for Zr(IV) and 60% for Mo(VI) at 2–3 M HNO_3, which corresponds to typical concentrations found in simulated HLLW. The adsorption ratio for Mo(VI) peaked at 0.1 M HNO_3 and then stabilized, indicating a change in the complexation mode of CMPO and Mo(VI) for HNO_3 concentrations between 0.1 and 1 M. For Zr(IV), the adsorption ratio increased with the HNO_3 concentration, likely due to the enhanced involvement of NO_3^- in complexation at higher concentrations.[15] This result suggests that controlling the HNO_3 concentration or selecting specific eluents may be key for optimizing the recovery of Zr(IV) and Mo(VI) from CMPO/SiO_2-P. Furthermore, high adsorption ratios for Re(VII) were observed at lower HNO_3 concentrations, reaching over 80% in 0.1 M HNO_3 solution.

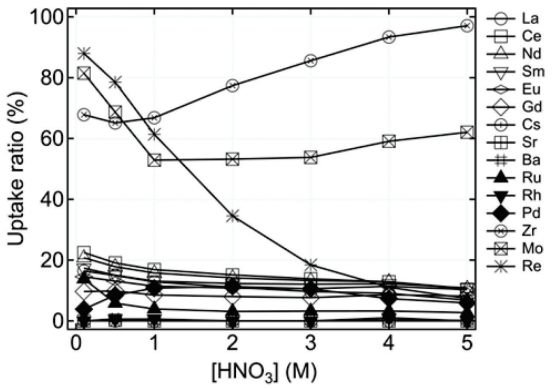

Fig. 3 Effect of HNO_3 concentration on the uptake ratio of 15 metal ions onto the CMPO/SiO_2-P adsorbent. [Metal] = 5 mM, [HNO_3] = 0.1–5 M, phase ratio: 0.2 g/4 mL, temperature: 25°C, contact time: 5 h

3. Adsorption Mechanism

(1) SEM-EDX and PIXE analyses

Figure 4 presents the X-ray spectra obtained from the PIXE and SEM-EDX analyses of the adsorbent after the batch experiment in a 2 M HNO_3 solution containing 10 mM Eu(III). Sharp peaks corresponding to Si and Al, attributable to the

SiO_2-P support, were observed in the spectra. Additionally, Fig. 4(a) shows peaks due to P in the CMPO adsorbent and peaks in the energy range of 5–10 keV ascribable to Eu(III). **Figure 5** displays the elemental map of the CMPO/SiO_2-P adsorbent after the batch adsorption experiment, which confirms that Eu(III) was uniformly distributed on the surface and inside the CMPO adsorbent after the adsorption process. These findings suggest that the CMPO extractant was uniformly grafted onto the SiO_2-P support during the synthesis process and metal ions were also adsorbed inside the CMPO/SiO_2-P adsorbent.

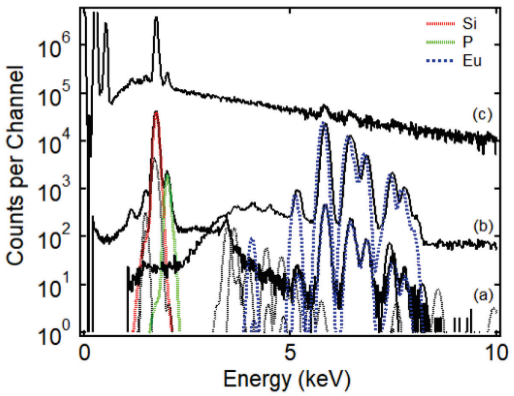

Fig. 4 X-ray spectra of the CMPO/SiO_2-P adsorbent after the batch adsorption experiment obtained via PIXE at (a) low energy and (b) high energy and (c) SEM-EDX

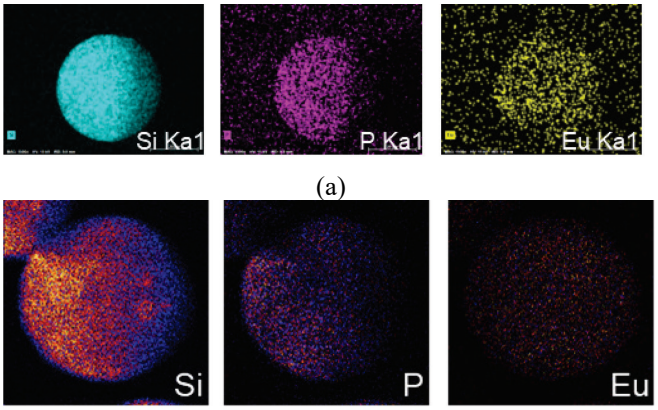

Fig. 5 Elemental maps of the CMPO/SiO_2-P adsorbent after the batch adsorption experiment obtained via (a) SEM and (b) PIXE

(2) XPS analysis

To further investigate the adsorption mechanism of metal ions on CMPO/SiO_2-P, a high-resolution XPS analysis was performed before and after Eu(III) adsorption, and the results are presented in Fig. 6. The wide-scan XPS spectrum of CMPO/SiO_2-P before adsorption exhibited strong peaks corresponding to N 1s, O 1s, C 1s, P 2p, Si 1s, and Si 2p, confirming that SiO_2, O, C, P, and N are the primary components of CMPO/SiO_2-P. After Eu(III) adsorption, a new sharp band associated with Eu 3d was detected. The high-resolution N 1s spectrum of the fresh resin displayed a single peak at 399.72 eV (C–N), consistent with the presence of a single type of N atoms in CMPO. After adsorption, a new band at 406.63 eV corresponding to Eu–NO_3 groups was observed, indicating that NO_3^- participates in the adsorption process. In the O 1s spectrum, peaks corresponding to P–O, Si–O, and C–O, which appeared initially at 533.34, 532.39, and 530.62 eV, respectively, were shifted after Eu(III) adsorption. According to the hard–soft acid–base theory[17], the Eu and O donors do not interact. However, the peak shift suggests that the P–O group in CMPO acts as a soft salt and interacts with Eu. Additionally, a pair of peaks representing Eu $3d_{5/2}$ and Eu $3d_{3/2}$ were detected, further confirming the adsorption of Eu(III) onto CMPO/SiO_2-P.

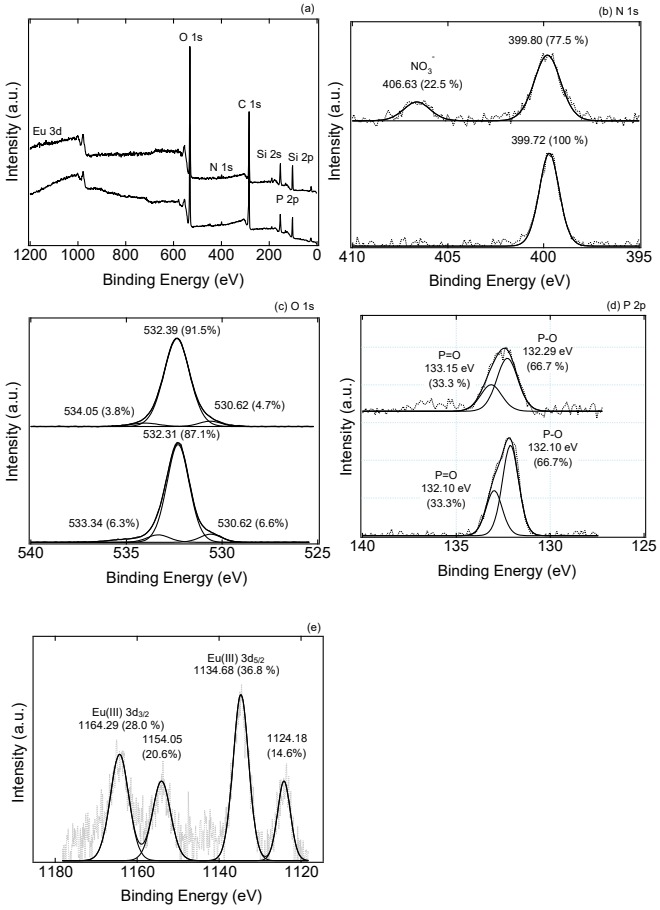

Fig. 6 XPS survey spectra of the CMPO/SiO_2-P adsorbent before (below) and after Eu(III) adsorption (above): (a) wide scan, (b) N 1s spectra, (c) O 1s spectra, (d) P 2p spectra, and (e) Eu 3d spectra

(3) Extraction of Eu(III) by CMPO

To elucidate the binding mode between the adsorbent and the metal, a slope analysis was conducted using batch experiments with an Eu concentration of 10 mM while varying the amount of adsorbent. The logarithmic plot of K_d calculated from the experimental results against the CMPO content in the adsorbent is presented in Fig. 7. The results revealed that the K_d of Eu increased proportionally with increasing CMPO/SiO_2-P content, with a slope of approximately 3, suggesting that the chemical bonding between CMPO and Eu can be expressed as follows:

$3CMPO/SiO_2\text{-}P + Eu^{3+} + 3NO_3^- \rightleftarrows Eu(NO_3)_3\cdot(CMPO/SiO_2\text{-}P)_3$

These results are consistent with previous studies on the behavior of CMPO in the solvent extraction of Ln(III)[18], implying a similar binding mode in the solid state.

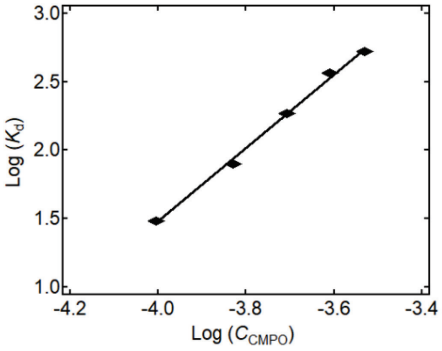

Fig. 7 Log distribution coefficient of Eu(III) versus log CMPO concentration. [Eu(III)] = 10 mM, [HNO_3] = 2 M, phase ratio: 0.2 g–0.6 g/4 mL, temperature: 25°C, contact time: 5 h

4. Column Experiment

A column experiment was conducted by passing a $^{241}Am/^{152}Eu$ mixed solution through CMPO/SiO_2–P. The results of the chromatogram obtained are shown in Fig. 8, and the recovery ratio and DF were calculated to confirm the recovery of Am, ^{152}Eu and Ln(III) and the retention of other elements in the adsorbent. After passing through 2 M HNO_3 as the washing solution, the nonadsorbed components Cs(I), Sr(II), Ba(II), Ru(III), Rh(III), Pd(II), and Re(VII) were quickly eluted. However, Pd(II) and Re(VII) eluted more slowly than other nonadsorbed components, affecting the water fraction of the eluent. Therefore, the contamination of the solution containing the target components can be prevented by adjusting the amount of washing solution. Next, ^{241}Am, ^{152}Eu, and Ln(III) were successfully co-recovered after passing water as the eluent.

Table 2 shows the recovery ratio for each element. First, the recovery ratio for ^{241}Am and ^{152}Eu and nonadsorbed components was almost 100%. For Zr(IV) and Mo(VI), the recovery ratio was 50%–60%, indicating that they were partially retained in the column, most likely due to the high adsorption efficiency of CMPO for these elements, as observed in the results of the HNO_3 concentration dependence. Since the retention of these elements may affect the reusability of the column, an appropriate eluent must be selected for their efficient recovery.

Table 2 shows the DF for each element. When the DF was calculated for the ^{241}Am product fraction (65-90ml) using H2O as the eluent, the nonadsorbed component Re(VII) was mixed into some of the product fractions, decreasing the DF. The presence of other elements may affect the selective separation of MA(III) from the MA(III) and Ln(III) solution. The DF results also revealed that adjusting the amount of cleaning solution is essential. Specifically, the DF of the MA(III)/Ln(III) solution is thought to be improved by increasing the amount of washing with 2M nitric acid or by increasing the column temperature to improve the elution rate of Re(VII).

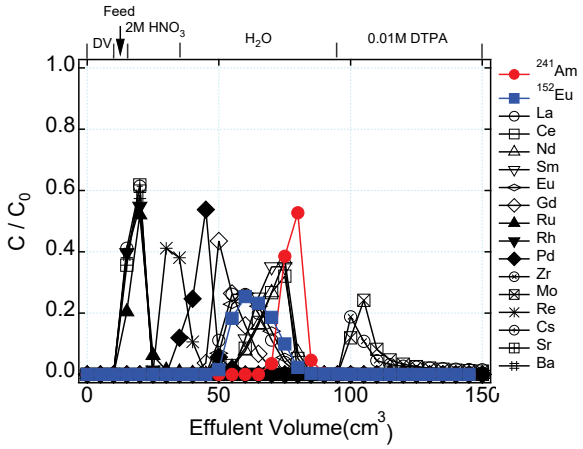

Fig. 8 Chromatographic separation results for the CMPO/SiO_2-P adsorbent

Table 2 Recovery ratios (R) and Decontamination factor (DF) of ^{241}Am, ^{152}Eu, and 15 other elements using the CMPO/SiO_2-P-packed column

	Feed 2M-HNO_3	Eluent H_2O	Eluent 0.01M-DTPA		
Element	R (%)	R (%)	R (%)	R (%)	DF
^{241}Am	-	99.8	0.12	100	1.00
^{152}Eu	-	99.8	0.12	100	3.19
La(III)	-	99.1	0.7	99.8	6.32
Ce(III)	-	92.4	-	92.4	1.55
Nd(III)	-	97.6	-	97.6	1.38
Sm(III)	-	100	-	100	1.41
Eu(III)	-	99.4	1.4	100	4.75
Gd(III)	-	98.3	-	98.3	51.1
Ru(III)	80	1.1	-	81.1	$>10^4$
Rh(III)	95.9	-	-	95.9	$>10^4$
Pd(II)	-	97.8	-	97.8	$>10^4$
Zr(IV)	-	-	52.4	52.4	$>10^4$
Mo(VI)	-	-	63.4	63.4	$>10^4$
Re(VII)	42	49.1	-	91.1	17.1
Cs(I)	100	-	-	100	$>10^4$
Sr(II)	97.4	-	-	97.4	$>10^4$
Ba(II)	97.4	-	-	97.4	$>10^4$

IV. Conclusion

The adsorption characteristics, binding modes with metals, and adsorption distribution of the CMPO/SiO_2-P adsorbent for MA(III) and Ln(III) were systematically investigated. In batch experiments, the adsorption ratio for Ln was constant at HNO_3 concentrations of 0.1–0.5 M, but the adsorption of Zr(IV), Mo(VI), and Re(VII) was affected by the HNO_3 concentration. Characterization of the adsorbent showed that the metal ions were adsorbed uniformly and that NO_3^- was involved in the binding of the extractant with metal ions. In column experiments using simulated solutions containing MA(III), the co-recovery ratio for MA(III) and Ln(III) was almost 100%, although the amount of washing solution and HNO_3 concentration must be optimized. Furthermore, high retention ratios in the column were observed for Zr(IV) and Mo(VI), indicating the possibility of mutual separation from

the MA(III)/Ln(III) group by appropriately controlling the eluent. The results of this study show that the CMPO/SiO_2-P adsorbent can be used to co-recover MA(III) and Ln(III) from HLLW containing high HNO_3 concentrations and various nuclides.

References

1) N. Apergis, J. E. Payne, K. Menyah, Y. Wolde-Rufael, "On the causal dynamics between emissions, nuclear energy, renewable energy, and economic growth," *Ecol Econ*, **69**[11], 2255-2260 (2010).
2) M. Abu-khader, "Recent advances in nuclear power: A review," *Prog Nucl Energ*, **51**[2], 225-235(2009)
3) S. A. Ansari, P. Pathak, P. K. Mohapatra, V. K. Manchanda, "Chemistry of diglycolamides: promising extractants for actinide partitioning," *Chem Rev*, **112**[3], 1751-1772 (2012)
4) S.-Y. Kim, Y. Xu, T. Ito, Y. Wu, T. Tada, K. Hitomi, E. Kuraoka, K. Ishii, "A novel partitioning process for treatment of high level liquid waste using macroporous silica-based adsorbents," *J Radioanal Nucl Chem*, **295**, 1043-1050 (2013)
5) J. Veliscek-Carolan, "Separation of actinides from spent nuclear fuel: A review," *J Hazard Mater*, **318**[15], 266-281 (2016)
6) Y. Zou,J. Li, S. Jia, S. WangY. SuK. Shi, T. Liu, J. Yang, X. Hou, J. He, "Separation of europium as a homologue of americium from high acidity solutions using a manufactured resin material," *Sep Purif Technol*, **340**, 126557 (2024)
7) Y. Horiuchi, S. Watanabe, Y. Sano, M. Takeuchi, F. Kida, T. Arai, "Development of MA separation process with TEHDGA/SiO_2-P for an advanced reprocessing," *J Radioanal Nucl Chem*, **330**[1], 237-244 (2021)
8) J. Chen, X. He, J. Wang, "Nuclear fuel cycle-oriented actinides separation in China," *Radiochimica Acta*, **102**[1-2], 41-45 (2014)
9) S. Ning, J. Zhou, S. Zhang, W. Zhang, Y. Wei, "Synthesis of soft N-donor iso Pentyl-BTBP and study on its removal of actinides from high level liquid waste," *Radiochimica Acta*, **108**[6], 425-431 (2020)
10) A. Zhang, Q. Hu, W. Wang, E. Kuraoka, "Application of a macroporous silica-based CMPO-impregnated polymeric composite in group partitioning of long-lived minor actinides from highly active liquid by extraction chromatography," *Ind Eng Chem Res*, **47** [16], 6158-6165 (2008).
11) S. Watanabe, T. Senzaki, A. Shibata, K. Nomura, M. Takeuchi, K. Nakatani, H. Matsuura, Y. Horiuchi, T. Arai, "Improvement in flow-sheet of extraction chromatography for trivalent minor actinides recovery," *J Radioanal Nucl Chem* **322**, 1273-1277 (2019)
12) S. Watanabe, Y. Sano, H. Shiwaku, T. Yaita, S. Ohno, T. Arai, H. Matsuura, M. Koka, T. Satoh, "Local structure and distribution of remaining elements inside extraction chromatography adsorbents," *Nucl Instrum Methods Phys Res Sect B*, **404**, 202-206 (2017)
13) N. Osawa, S.-Y. Kim, M. Kubota, H. Wu, S. Watanabe, T. Ito, R. Nagaishi, "Adsorption behavior of platinum-group metals and Co-existing metal ions from simulated high-level liquid waste using HONTA and Crea impregnated adsorbent," *Nucl Eng Technol*, **56**[3], 812-818 (2024)
14) M. Kubota, S.-Y. Kim, H. Wu, S. Watanabe, Y. Sano, M. Takeuchi, T. Arai, "Development of a process for the separation of MA (III) from Ln (III) fission products using HONTA impregnated adsorbent," *J Radioanal Nucl Chem*, **333**[5], 2413-2420 (2024)
15) A. Zhang, Y. Wei, M. Kumagai, "Properties and mechanism of molybdenum and zirconium adsorption by a macroporous silica-based extraction resin in the MAREC process," *Solv Extr Ion Exch*, **21**[4], 591-611 (2007)
16) T. Ho, "Hard soft acids bases (HSAB) principle and organic chemistry," *Chem Rev*, **75**[1], 1-20 (1975)
17) S. Belair, C. Lamouroux, M. Tabarant, A. Labet, C. Mariet, P. Dannus, "Modeling of the extraction of lanthanide nitrates from aqueous solutions over a wide range of activities by CMPO," *Solv Extr Ion Exch*, **22**[5], 791-811 (2004).